

Quantum effects on dynamic structure factors in dense magnetized plasmas

Tushar Mondal^{1,*} and Gianluca Gregori^{2,†}

¹*International Centre for Theoretical Sciences, Tata Institute of Fundamental Research, Bengaluru 560089, India*

²*Department of Physics, University of Oxford, Parks Road, Oxford OX1 3PU, United Kingdom*



(Received 19 October 2023; accepted 6 December 2023; published 24 January 2024)

We extend the classical magnetohydrodynamics formalism to include nonlocal quantum behavior via the phenomenological Bohm potential. We then solve the quantum magnetohydrodynamics equations to obtain a new analytical form of the dynamic structure factor (DSF), a fundamental quantity linking theory and experiments. Our results show that the three-peak structure—one central Rayleigh peak and two Brillouin peaks—of the DSF arising from quantum hydrodynamic fluctuations becomes (in general) a five-peak structure—one central Rayleigh peak and two pairs of peaks associated with fast and slow magnetosonic waves. The Bohm contribution influences the positions and characteristics (height, width, and intensity) of the peaks by introducing three significant modifications: (i) an increase in effective thermal pressure, (ii) a reduction in the adiabatic index, and (iii) an enhancement of effective thermal diffusivity. The multiple DSF peaks enable concurrent measurements of diverse plasma properties, transport coefficients, and thermodynamic parameters in magnetized dense plasmas. The potential for experimental validation of our theory looms large, particularly through future experiments conducted at state-of-the-art laser facilities.

DOI: [10.1103/PhysRevResearch.6.013089](https://doi.org/10.1103/PhysRevResearch.6.013089)

I. INTRODUCTION

In the universe, matter is often found in extreme states, with densities comparable to solids and temperatures of a few electron volts, known as warm dense matter (WDM). As the temperature rises to the order of a few keV, one enters the regime of a hot dense plasma. Matter under such extreme conditions is characterized by partially degenerate electrons and strongly correlated ions [1,2]. Precise measurements of plasma conditions, including transport and thermodynamic properties in both WDM and dense plasmas, are of high importance for understanding high-energy density physics phenomena. The applications span a wide range, from modeling the atmosphere of neutron stars [3] and magnetars [4,5] to investigating the interiors of giant planets [6,7], white [8,9] and brown dwarfs [10], as well as for the advancement of inertial confinement fusion [11,12], with its promise of potentially abundant and clean energy for the future. However, the extreme conditions pose significant challenges in diagnostics, often preventing direct measurement of even basic plasma properties.

A fundamental quantity that describes the microscopic space- and time-dependent behavior of WDM and dense plasmas is the dynamic structure factor (DSF) [13]. The DSF contains essential information on the energy and angular distribution of the scattering that results from the individual

and collective behavior of electrons and ions. This property, in turn, makes the DSF a function of macroscopic plasma quantities such as density, temperature, and magnetic fields. Since the DSF is directly proportional to the x-ray Thomson scattering cross section, it can be probed through laser plasma experiments [14]. The comparison between experimental and calculated DSF not only validates theoretical models but also allows the simultaneous measurement of plasma properties that are otherwise challenging to determine. Thus, the DSF serves as a powerful diagnostic tool for probing, understanding, and characterizing the intricate behavior of WDM and dense plasmas, making a significant contribution to the advancement of high-energy density physics research.

The DSF is formally defined as the Fourier transform in space and time of the density autocorrelation function. For density fluctuations, the hydrodynamic description is highly successful due to its analytical solvability [13], connecting fundamental thermodynamics and transport properties of plasmas in a simple physical form. These analytical results have shown good agreement with molecular dynamic simulations [15,16] in predicting the dynamical response of strongly coupled classical plasmas. However, classical hydrodynamics falls short in capturing various astrophysical and laboratory conditions, such as systems with dynamically dominant magnetic fields and quantum effects. In the presence of a background magnetic field, previous results have been limited to special cases like weakly coupled plasmas [17,18] or those neglecting particle correlations [19]. Recently, Bott and Gregori [20] computed the DSF in a magnetized, high-density plasma, describing collective excitations through magnetohydrodynamics (MHD).

In this paper, we extend the classical MHD formalism to incorporate quantum effects through the introduction of the Bohm potential [21–24]. This novel approach allows

*tushar.mondal@icts.res.in

†gianluca.gregori@physics.ox.ac.uk

Published by the American Physical Society under the terms of the Creative Commons Attribution 4.0 International license. Further distribution of this work must maintain attribution to the author(s) and the published article's title, journal citation, and DOI.

us to derive an analytical expression for the modified DSF in strongly coupled, partially degenerate, and magnetized plasmas. Our comprehensive framework encompasses finite viscosity, thermal conductivity, electrical resistivity, and quantum nonlocality. We demonstrate that quantum effects do not change the number of excitation modes compared to their classical counterparts. However, we will show that the introduction of quantum contributions leads to substantial modifications in the positions and characteristics of these DSF resonances through (i) a significant enhancement of effective thermal pressure, (ii) a reduction in the adiabatic index, and (iii) an augmentation of effective thermal diffusivity.

Traditionally, the Landau-Placzek ratio [13], defined as the ratio of the Rayleigh peak intensity to that of the two Brillouin peaks, offers a means to estimate the specific heat ratio (adiabatic index) of fluids across a wide range of thermodynamic conditions [25–28]. In quantum MHD, we demonstrate that the expression for the Landau-Placzek ratio remains unchanged as $R_{LP} = \gamma' - 1$, with the adiabatic index γ being modified due to the Bohm contributions. Additionally, we introduce another significant parameter, the F-to-S ratio, which quantifies the intensity ratio of the fast magnetosonic wave peak to the slow magnetosonic wave peak. This ratio provides an experimental avenue for measuring the magnetic field strength within the plasma medium.

The paper is organized as follows. In Sec. II, we present the governing equations of MHD in a standard form, incorporating quantum dynamics through the Bohm potential. Section III provides a derivation of the density autocorrelation function, and consequently, the dynamic structure factor, within the context of quantum MHD for small-amplitude fluctuations. Moving on to Sec. IV, we derive the general form of the dynamic structure factor for fluctuations with wave vectors parallel to the magnetic field. This scenario closely resembles quantum hydrodynamics fluctuations. In Sec. V, we extend our analysis to derive the general form of the dynamic structure factor for oblique fluctuations within the quantum MHD framework. Finally, the paper concludes with a summary in Sec. VI.

II. GENERAL MAGNETOHYDRODYNAMICS EQUATIONS

We systematically present the general set of single-fluid MHD equations governing an electron-ion plasma, incorporating considerations of heat conduction and quantum effects. The ideal quantum MHD equations are derived from the first-principles kinetic description of quantum plasmas [29]. In contrast, the relevant transport coefficients, essential for a comprehensive description of the system, are derived from classical kinetic theory [30]. Generalizing them to quantum, nonideal plasmas is not a trivial task, and in the context of this work, such coefficients must be assumed to provide only a phenomenological description of the plasma. On the other hand, if experimental data becomes available, the phenomenological description used here can be employed to extract those coefficients from the data itself.

The governing equations for the conservation of mass, momentum, magnetic flux, and internal energy are given,

respectively, by [31]

$$\frac{d\rho}{dt} = -\rho \nabla \cdot \mathbf{u}, \quad (1a)$$

$$\rho \frac{d\mathbf{u}}{dt} = -\nabla p - \nabla \cdot \mathbf{\Pi} + \frac{(\nabla \times \mathbf{B}) \times \mathbf{B}}{\mu_0} + \mathbf{\Phi}_{\text{Bohm}}, \quad (1b)$$

$$\frac{d\mathbf{B}}{dt} = (\mathbf{B} \cdot \nabla) \mathbf{u} - \mathbf{B}(\nabla \cdot \mathbf{u}) - \nabla \times (\eta \nabla \times \mathbf{B}), \quad (1c)$$

$$\rho \frac{d\epsilon}{dt} = -p \nabla \cdot \mathbf{u} - \mathbf{\Pi} : \nabla \mathbf{u} + \eta \frac{|\nabla \times \mathbf{B}|^2}{\mu_0} - \nabla \cdot \mathbf{q} + \mathbf{\Phi}_{\text{Bohm}} \cdot \mathbf{u}, \quad (1d)$$

where ρ is the mass density, t the time, \mathbf{u} the bulk fluid velocity, p the pressure, $\mathbf{\Pi}$ the viscosity tensor, $\mathbf{\Phi}_{\text{Bohm}}$ the quantum Bohm potential, \mathbf{B} the magnetic field, μ_0 the permeability of free space, η the magnetic diffusivity, ϵ the internal energy, and \mathbf{q} is the heat flux. Here, the convective derivative can be written as $d/dt \equiv \partial/\partial t + \mathbf{u} \cdot \nabla$. The expressions for the viscosity tensor, heat flux, and the quantum Bohm potential (see Appendix A for more detail) are explicitly given by [31]

$$\mathbf{\Pi} = -\zeta_s \left[\nabla \mathbf{u} + (\nabla \mathbf{u})^T - \frac{2}{3} (\nabla \cdot \mathbf{u}) \mathbf{I} \right] - \zeta_b (\nabla \cdot \mathbf{u}) \mathbf{I}, \quad (2a)$$

$$\mathbf{q} = -\kappa \nabla T, \quad (2b)$$

$$\mathbf{\Phi}_{\text{Bohm}} = \frac{\hbar^2 \rho}{2m_e m_i} \nabla \left(\frac{\nabla^2 \sqrt{\rho}}{\sqrt{\rho}} \right), \quad (2c)$$

where ζ_s is the shear viscosity (or the first coefficient of viscosity), ζ_b the bulk viscosity (or the second coefficient of viscosity), \mathbf{I} the identity tensor, κ the thermal conductivity, T the fluid temperature, \hbar the reduced Planck's constant, m_e the electron mass, and m_i the ion mass. Note that the momentum associated with a fluid element can change not only by the pressure gradient and the inertial term but also because of viscous drag, the Lorentz force, and quantum effects arising from the contribution of the Bohm potential. The energy equation correctly describes the nonlocal quantum effects as well as the effects arising from the nonideal heat flux.

It is worth rewriting the internal energy conservation law (1d) as a temperature evolution equation in terms of density, bulk flow velocity, and the magnetic field. Following the first law of thermodynamics, and using thermodynamic identities and Eq. (1a), we can rewrite Eq. (1d) as (see Appendix B for details)

$$\rho C_V \frac{dT}{dt} = -\frac{\gamma - 1}{\alpha_T} \rho C_V \nabla \cdot \mathbf{u} - \mathbf{\Pi} : \nabla \mathbf{u} + \eta \frac{|\nabla \times \mathbf{B}|^2}{\mu_0} - \nabla \cdot \mathbf{q} + \mathbf{\Phi}_{\text{Bohm}} \cdot \mathbf{u}, \quad (3)$$

where C_V is the heat capacity at constant volume, γ the adiabatic index, and α_T the coefficient of thermal expansion. Also, we eliminate the pressure gradient in Eq. (1b) using the thermodynamic identity (see Appendix B for details)

$$\nabla p = \frac{c_s^2}{\gamma} (\nabla \rho + \rho \alpha_T \nabla T), \quad (4)$$

where c_s is the adiabatic sound speed.

On substituting (2) and (4), we rewrite the set of MHD equations as

$$\frac{d\rho}{dt} = -\rho \nabla \cdot \mathbf{u}, \quad (5a)$$

$$\begin{aligned} \rho \frac{d\mathbf{u}}{dt} = & -\frac{c_s^2}{\gamma} (\nabla \rho + \rho \alpha_T \nabla T) + \frac{(\nabla \times \mathbf{B}) \times \mathbf{B}}{\mu_0} \\ & + \Phi_{\text{Bohm}} + \nabla (\zeta_b \nabla \cdot \mathbf{u}) \\ & + \nabla \cdot \left[\zeta_s \left\{ \nabla \mathbf{u} + (\nabla \mathbf{u})^T - \frac{2}{3} (\nabla \cdot \mathbf{u}) \mathbf{I} \right\} \right], \end{aligned} \quad (5b)$$

$$\frac{d\mathbf{B}}{dt} = (\mathbf{B} \cdot \nabla) \mathbf{u} - \mathbf{B} (\nabla \cdot \mathbf{u}) - \nabla \times (\eta \nabla \times \mathbf{B}), \quad (5c)$$

$$\begin{aligned} \rho \frac{dT}{dt} = & -\frac{\gamma-1}{\alpha_T} \rho \nabla \cdot \mathbf{u} - \frac{1}{C_V} \mathbf{\Pi} : \nabla \mathbf{u} + \eta \frac{|\nabla \times \mathbf{B}|^2}{\mu_0 C_V} \\ & + \frac{1}{C_V} \nabla \cdot (\kappa \nabla T) + \frac{1}{C_V} \Phi_{\text{Bohm}} \cdot \mathbf{u}. \end{aligned} \quad (5d)$$

In the temperature evolution equation, we have not written down the full expression for viscous dissipation term for brevity.

III. FLUCTUATIONS AND THE DYNAMIC STRUCTURE FACTOR

We now focus on the calculation of the density autocorrelation function, and thereby the quantum-MHD dynamic structure factor in the limit of small-amplitude fluctuations. To perform this calculation, we consider small fluctuations of dynamic quantities for a fluid system in some equilibrium state, and linearize the above quantum-MHD equations. We assume the system is in equilibrium at a density ρ_0 , bulk flow velocity $\mathbf{u}_0 = 0$, magnetic field \mathbf{B}_0 , temperature T_0 , sound speed c_{s0} , adiabatic index γ_0 , coefficient of thermal expansion α_{T0} , specific heat capacity at constant volume C_{V0} , thermal conductivity κ_0 , bulk viscosity ζ_{b0} , shear viscosity ζ_{s0} , and magnetic diffusivity η_0 . We then take the small-amplitude fluctuations of dynamic quantities on this equilibrium state, as

$$\rho = \rho_0 + \delta\rho, \quad \mathbf{u} = \delta\mathbf{u}, \quad \mathbf{B} = \mathbf{B}_0 + \delta\mathbf{B}, \quad T = T_0 + \delta T. \quad (6)$$

Substituting linearization (6) into Eqs. (5a)–(5d), and neglecting terms quadratic or higher order in fluctuating quantities, we obtain

$$\frac{\partial \delta\rho}{\partial t} = -\rho_0 \nabla \cdot \delta\mathbf{u}, \quad (7a)$$

$$\begin{aligned} \rho_0 \frac{\partial \delta\mathbf{u}}{\partial t} = & -\frac{c_{s0}^2}{\gamma_0} (\nabla \delta\rho + \rho_0 \alpha_{T0} \nabla \delta T) + \frac{\mathbf{B}_0 \cdot \nabla \delta\mathbf{B}}{\mu_0} \\ & - \nabla \cdot \left(\frac{\mathbf{B}_0 \cdot \delta\mathbf{B}}{\mu_0} \right) + \zeta_{s0} \nabla^2 \delta\mathbf{u} + \zeta_{c0} \nabla (\nabla \cdot \delta\mathbf{u}) \\ & + \frac{\hbar^2}{4m_e m_i} \nabla (\nabla^2 \delta\rho), \end{aligned} \quad (7b)$$

$$\frac{\partial \delta\mathbf{B}}{\partial t} = \mathbf{B}_0 \cdot \nabla \delta\mathbf{u} - \mathbf{B}_0 \nabla \cdot \delta\mathbf{u} + \eta_0 \nabla^2 \delta\mathbf{B}, \quad (7c)$$

$$\frac{\partial \delta T}{\partial t} = -\frac{\gamma_0 - 1}{\alpha_{T0}} \nabla \cdot \delta\mathbf{u} + \gamma_0 \chi_0 \nabla^2 \delta T, \quad (7d)$$

where we have defined the compressive viscosity coefficient $\zeta_{c0} \equiv \zeta_{b0} - 2\zeta_{s0}/3$, and thermal diffusivity $\chi_0 \equiv \kappa_0/\rho_0 C_{V0} \gamma_0$. Here, the terms with subscript 0 refer to the quantities at equilibrium.

To obtain the MHD DSF, we apply to Eqs. (7a)–(7d) a Laplace transform in time, and a Fourier transform in space. For any plasma quantity δx , this operation is defined as

$$\tilde{\delta x}_k(s) = \int_0^\infty dt e^{-st} \int_{-\infty}^{+\infty} d^3r e^{ik \cdot r} \delta x(\mathbf{r}, t),$$

where the quantity with tilde indicates the transformed one, and $s = \epsilon + i\omega$ is the complex Laplace variable. Using standard properties of Fourier and Laplace transforms under derivatives, we find

$$s \tilde{\delta \rho}_k(s) = -i \rho_0 \mathbf{k} \cdot \tilde{\delta \mathbf{u}}_k(s) + \delta \rho_k(0), \quad (8a)$$

$$\begin{aligned} \rho_0 s \tilde{\delta \mathbf{u}}_k(s) = & -\frac{c_{s0}^2}{\gamma_0} [i \mathbf{k} \tilde{\delta \rho}_k(s) + i \rho_0 \alpha_{T0} \mathbf{k} \tilde{\delta T}_k(s)] \\ & + i \tilde{\delta \mathbf{B}}_k(s) \frac{\mathbf{B}_0 \cdot \mathbf{k}}{\mu_0} - i \mathbf{k} \frac{\mathbf{B}_0 \cdot \tilde{\delta \mathbf{B}}_k(s)}{\mu_0} \\ & - \zeta_{s0} k^2 \tilde{\delta \mathbf{u}}_k(s) - \zeta_{c0} \mathbf{k} [\mathbf{k} \cdot \tilde{\delta \mathbf{u}}_k(s)] \\ & - \frac{\hbar^2 k^2}{4m_e m_i} i \mathbf{k} \tilde{\delta \rho}_k(s) + \rho_0 \delta \mathbf{u}_k(0), \end{aligned} \quad (8b)$$

$$\begin{aligned} s \tilde{\delta \mathbf{B}}_k(s) = & i (\mathbf{B}_0 \cdot \mathbf{k}) \tilde{\delta \mathbf{u}}_k(s) - i \mathbf{B}_0 [\mathbf{k} \cdot \tilde{\delta \mathbf{u}}_k(s)] \\ & - \eta_0 k^2 \tilde{\delta \mathbf{B}}_k(s) + \delta \mathbf{B}_k(0), \end{aligned} \quad (8c)$$

$$s \tilde{\delta T}_k(s) = -i \frac{\gamma_0 - 1}{\alpha_{T0}} \mathbf{k} \cdot \tilde{\delta \mathbf{u}}_k(s) - \gamma_0 \chi_0 k^2 \tilde{\delta T}_k(s) + \delta T_k(0). \quad (8d)$$

A. Density autocorrelation function

We assume that the initial density fluctuations $\delta \rho_k(0)$ are uncorrelated with the initial velocity fluctuations $\delta \mathbf{u}_k(0)$, the initial magnetic field fluctuations $\delta \mathbf{B}_k(0)$, and the initial temperature fluctuations $\delta T_k(0)$. This assumption allows $\delta \mathbf{u}_k(0)$, $\delta \mathbf{B}_k(0)$, and $\delta T_k(0)$ to be set to zero. Next, we write the magnetic field fluctuations $\tilde{\delta \mathbf{B}}_k(s)$ and the temperature fluctuations $\tilde{\delta T}_k(s)$ in terms of velocity field fluctuations $\tilde{\delta \mathbf{u}}_k(s)$, using Eqs. (8c) and (8d), respectively:

$$\tilde{\delta \mathbf{B}}_k(s) = \frac{i(\mathbf{k} \cdot \mathbf{B}_0) \tilde{\delta \mathbf{u}}_k(s) - i[\mathbf{k} \cdot \tilde{\delta \mathbf{u}}_k(s)] \mathbf{B}_0}{s + \eta_0 k^2}, \quad (9a)$$

$$\tilde{\delta T}_k(s) = -\frac{i(\gamma_0 - 1)[\mathbf{k} \cdot \tilde{\delta \mathbf{u}}_k(s)]}{\alpha_{T0}(s + \gamma_0 \chi_0 k^2)}. \quad (9b)$$

We then solve for $\mathbf{B}_0 \cdot \tilde{\delta \mathbf{u}}_k(s)$ in terms of $\tilde{\delta \rho}_k(s)$ and $i \rho_0 \mathbf{k} \cdot \tilde{\delta \mathbf{u}}_k(s)$, by taking the scalar product of (8b) with \mathbf{B}_0 , and

substituting (9b). This gives

$$\mathbf{B}_0 \cdot \widetilde{\delta \mathbf{u}}_k(s) = -\frac{i(\mathbf{k} \cdot \mathbf{B}_0)}{(\rho_0 s + \zeta_{s0} k^2)} \left[\left(\frac{c_{s0}^2}{\gamma_0} + \frac{\hbar^2 k^2}{4m_e m_i} \right) \widetilde{\delta \rho}_k(s) - \left\{ \frac{(\gamma_0 - 1)c_{s0}^2}{\gamma_0(s + \gamma_0 \chi_0 k^2)} + v_{c0} \right\} i\rho_0 \mathbf{k} \cdot \widetilde{\delta \mathbf{u}}_k(s) \right]. \quad (10)$$

We subsequently evaluate $i\rho_0 \mathbf{k} \cdot \widetilde{\delta \mathbf{u}}_k(s)$ in terms of $\widetilde{\delta \rho}_k(s)$ alone, using the scalar product between (8b) and $i\mathbf{k}$, as well as substituting (9a), (9b), and (10):

$$i\rho_0 \mathbf{k} \cdot \widetilde{\delta \mathbf{u}}_k(s) = \left(\frac{k^2 c_{s0}^2}{\gamma_0} + \frac{\hbar^2 k^4}{4m_e m_i} \right) \left[1 + \frac{(\mathbf{k} \cdot \mathbf{B}_0)^2}{\mu_0(s + \eta_0 k^2)(\rho_0 s + \zeta_{s0} k^2)} \right] \widetilde{\delta \rho}_k(s) - \left[\frac{(\gamma_0 - 1)k^2 c_{s0}^2}{\gamma_0(s + \gamma_0 \chi_0 k^2)} + v_{l0} k^2 \right. \\ \left. + \frac{k^2 B_0^2}{\mu_0 \rho_0(s + \eta_0 k^2)} + \frac{k^2 (\mathbf{k} \cdot \mathbf{B}_0)^2}{\mu_0(s + \eta_0 k^2)(\rho_0 s + \zeta_{s0} k^2)} \left\{ \frac{(\gamma_0 - 1)c_{s0}^2}{\gamma_0(s + \gamma_0 \chi_0 k^2)} + v_{c0} \right\} \right] i\rho_0 \mathbf{k} \cdot \widetilde{\delta \mathbf{u}}_k(s). \quad (11)$$

After some rearrangement, this gives

$$i\rho_0 \mathbf{k} \cdot \widetilde{\delta \mathbf{u}}_k(s) = \left[\frac{D(k, s)}{N(k, s)} - s \right] \widetilde{\delta \rho}_k(s), \quad (12)$$

where the functions $N(k, s)$ and $D(k, s)$ are defined as

$$N(k, s) = (s + \gamma_0 \chi_0 k^2)(s + v_{l0} k^2)(s + \eta_0 k^2)(s + v_{s0} k^2) \\ + \frac{\gamma_0 - 1}{\gamma_0} k^2 c_{s0}^2 (s + \eta_0 k^2)(s + v_{s0} k^2) \\ + k^2 v_A^2 (s + \gamma_0 \chi_0 k^2) [s + k^2 (v_{s0} + v_{c0} \cos^2 \theta)] \\ + \frac{\gamma_0 - 1}{\gamma_0} k^4 v_A^2 c_{s0}^2 \cos^2 \theta, \quad (13a)$$

$$D(k, s) = \left(\frac{k^2 c_{s0}^2}{\gamma_0} + \frac{\hbar^2 k^4}{4m_e m_i} \right) (s + \gamma_0 \chi_0 k^2) \\ \times [(s + \eta_0 k^2)(s + v_{s0} k^2) + k^2 v_A^2 \cos^2 \theta] \\ + sN(k, s). \quad (13b)$$

Here, we define various additional quantities: shear kinematic viscosity $v_{s0} \equiv \zeta_{s0}/\rho_0$, compressive kinematic viscosity $v_{c0} = \zeta_{c0}/\rho_0$, longitudinal kinematic viscosity $v_{l0} = v_{s0} + v_{c0}$, θ the angle between \mathbf{B}_0 and \mathbf{k} , and $v_A \equiv B_0/\sqrt{\mu_0 \rho_0}$ the Alfvén speed, where $B_0 = |\mathbf{B}_0|$.

Finally, we substitute (12) into (8a), and solve for $\widetilde{\delta \rho}_k(s)$ in terms of $\delta \rho_k(0)$,

$$\widetilde{\delta \rho}_k(s) = \frac{N(k, s)}{D(k, s)} \delta \rho_k(0). \quad (14)$$

It provides the density autocorrelation function:

$$\frac{\langle \delta \rho_k^*(0) \widetilde{\delta \rho}_k(s) \rangle}{\langle \delta \rho_k^*(0) \delta \rho_k(0) \rangle} = \frac{N(k, s)}{D(k, s)}. \quad (15)$$

B. Dynamic structure factor

The dynamic structure factor $S_{nn}(\mathbf{k}, \omega)$ is [20]

$$\frac{2\pi S_{nn}(\mathbf{k}, \omega)}{S_{nn}(\mathbf{k})} = 2\text{Re} \left[\lim_{\varepsilon \rightarrow 0} \frac{\langle \delta \rho_k^*(0) \widetilde{\delta \rho}_k(s = \varepsilon + i\omega) \rangle}{\langle \delta \rho_k^*(0) \delta \rho_k(0) \rangle} \right], \quad (16)$$

where

$$S_{nn}(\mathbf{k}) = \int S_{nn}(\mathbf{k}, \omega) d\omega, \quad (17)$$

is the static structure factor.

IV. PARALLEL FLUCTUATIONS

We first consider fluctuations whose wave vector is parallel to the magnetic field, i.e., $\cos \theta = 1$. In this case, we have

$$N(k, s) = [(s + \eta_0 k^2)(s + v_{s0} k^2) + k^2 v_A^2] N_{\parallel}(k, s), \quad (18a)$$

$$D(k, s) = [(s + \eta_0 k^2)(s + v_{s0} k^2) + k^2 v_A^2] D_{\parallel}(k, s), \quad (18b)$$

where

$$N_{\parallel}(k, s) = (s + \gamma_0 \chi_0 k^2)(s + v_{l0} k^2) + \frac{\gamma_0 - 1}{\gamma_0} k^2 c_{s0}^2, \quad (19a)$$

$$D_{\parallel}(k, s) = \left(\frac{k^2 c_{s0}^2}{\gamma_0} + \frac{\hbar^2 k^4}{4m_e m_i} \right) (s + \gamma_0 \chi_0 k^2) \\ + sN_{\parallel}(k, s). \quad (19b)$$

The density autocorrelation function becomes

$$\frac{\langle \delta \rho_k^*(0) \widetilde{\delta \rho}_k(s) \rangle}{\langle \delta \rho_k^*(0) \delta \rho_k(0) \rangle} = \frac{N_{\parallel}(k, s)}{D_{\parallel}(k, s)}. \quad (20)$$

First, neglecting all the diffusive effects, we find

$$N_{\parallel}(k, s) = s^2 + \frac{\gamma_0 - 1}{\gamma_0} k^2 c_{s0}^2, \quad (21a)$$

$$D_{\parallel}(k, s) = s \left(s^2 + k^2 c_{s0}^2 + \frac{\hbar^2 k^4}{4m_e m_i} \right). \quad (21b)$$

The roots are then

$$s_* = 0, \quad \pm i k c_{\text{eff}}, \quad (22)$$

where

$$c_{\text{eff}} = \sqrt{c_{s0}^2 + c_Q^2}, \quad \text{with } c_Q^2 = \frac{\hbar^2 k^2}{4m_e m_i}. \quad (23)$$

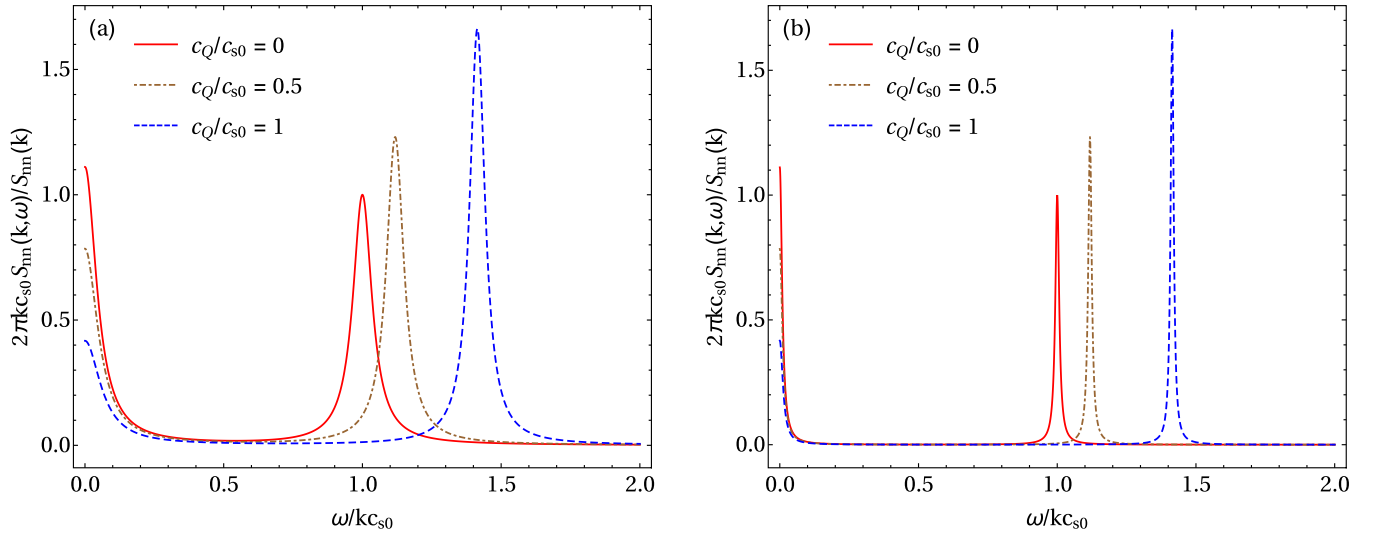


FIG. 1. The dynamic structure factor in magnetized, high-density plasma with increasing quantum effects at $\theta = 0^\circ$. The structure factor is presented in a dimensionless form; this is obtained via $s \mapsto skc_{s0}$. With this mapping, the magnitude of the various dissipative terms are represented by the dimensionless numbers $k\chi_0/c_{s0}$, $k\eta_0/c_{s0}$, kv_{s0}/c_{s0} , and kv_{c0}/c_{s0} . The peak magnitude is normalized to the classical ($c_Q/c_{s0} = 0$), parallel case. We choose $\gamma_0 = 5/3$. The dimensionless values of the dissipative terms: (a) $k\chi_0/c_{s0} = 0.05$, $k\eta_0/c_{s0} = 0.05$, $kv_{s0}/c_{s0} = 0.0335$ and $kv_{c0}/c_{s0} = 0.0165$, and (b) $k\chi_0/c_{s0} = 0.01$, $k\eta_0/c_{s0} = 0.01$, $kv_{s0}/c_{s0} = 0.0067$ and $kv_{c0}/c_{s0} = 0.0033$.

We then determine the density autocorrelation function in the neighborhood of each of these roots in turn. The numerator is $N(k, s_*) \neq 0$ in each case. By reintroducing the diffusive terms, we have [20]

(1) $s_* = 0$: Let $s = \delta s \sim \chi_0 k^2, \eta_0 k^2, v_{s0} k^2, v_{l0} k^2$. Then,

$$D_{\parallel}(k, s) \approx k^2 c_{s0}^2 (\delta s + \chi_0 k^2) + k^2 c_Q^2 (\delta s + \gamma_0 \chi_0 k^2),$$

$$\frac{\langle \delta \rho_{\mathbf{k}}^*(0) \widetilde{\delta \rho_{\mathbf{k}}}(s) \rangle}{\langle \delta \rho_{\mathbf{k}}^*(0) \delta \rho_{\mathbf{k}}(0) \rangle} \approx \frac{(\gamma_0 - 1) c_{s0}^2 / (\gamma_0 c_{\text{eff}}^2)}{s + \Gamma_{\chi} k^2}, \quad (24)$$

where

$$\Gamma_{\chi} = \frac{c_{s0}^2 + \gamma_0 c_Q^2}{c_{\text{eff}}^2} \chi_0 = Q \chi_0, \quad (25)$$

and

$$Q = \frac{c_{s0}^2 + \gamma_0 c_Q^2}{c_{\text{eff}}^2} \geq 1. \quad (26)$$

In the classical limit (i.e., $c_Q = 0$), the factor Q becomes unity.

(2) $s_* = \pm ikc_{\text{eff}}$: Let $s = \pm ikc_{\text{eff}} + \delta s$, $\delta s \sim \chi_0 k^2, \eta_0 k^2, v_{s0} k^2, v_{l0} k^2$. Then,

$$D_{\parallel}(k, s) \approx -2k^2 c_{\text{eff}}^2 (\delta s + \Gamma_{\parallel} k^2),$$

where

$$\Gamma_{\parallel} = \frac{1}{2} (v_{l0} + \gamma_0 \chi_0 - \Gamma_{\chi}). \quad (27)$$

It follows that

$$\frac{\langle \delta \rho_{\mathbf{k}}^*(0) \widetilde{\delta \rho_{\mathbf{k}}}(s) \rangle}{\langle \delta \rho_{\mathbf{k}}^*(0) \delta \rho_{\mathbf{k}}(0) \rangle} \approx \frac{(\gamma_0 c_Q^2 + c_{s0}^2) / (2\gamma_0 c_{\text{eff}}^2)}{s \mp ikc_{\text{eff}} + \Gamma_{\parallel} k^2}. \quad (28)$$

The dynamic structure factor can be derived using (16):

$$\frac{2\pi S_{nn}(k, \omega)}{S_{nn}(k)} \approx \frac{\gamma_0 - 1}{\gamma_0} \frac{c_{s0}^2}{c_{\text{eff}}^2} \left[\frac{2\Gamma_{\chi} k^2}{\omega^2 + (\Gamma_{\chi} k^2)^2} \right]$$

$$+ \frac{Q}{\gamma_0} \left[\frac{\Gamma_{\parallel} k^2}{(\Gamma_{\parallel} k^2)^2 + (\omega + c_{\text{eff}} k)^2} \right]$$

$$+ \frac{\Gamma_{\parallel} k^2}{(\Gamma_{\parallel} k^2)^2 + (\omega - c_{\text{eff}} k)^2}. \quad (29)$$

The dynamic structure factors for parallel modes are shown in Fig. 1 for different values of c_Q/c_{s0} . The calculated structure factor is similar to the hydrodynamic structure factor with some modifications arising from the contribution of the Bohm potential. In MHD, parallel fluctuations of magnetic fields propagate as the Alfvén waves and do not have a density perturbation associated with them. Since the parallel compressive fluctuations do not interact with the magnetic fields, the MHD structure factor for parallel wave numbers becomes identical to the hydrodynamic one. The spectrum consists of three peaks: the central Rayleigh peak at $\omega = 0$, and two Brillouin peaks at $\omega = \pm kc_{\text{eff}}$. The physical nature of two different peaks can be explained qualitatively through the thermodynamic theory of fluctuations. Since the sound propagation is an adiabatic process, the density fluctuations can be decomposed into two types: entropy fluctuation at constant pressure and pressure fluctuation at constant entropy. The Rayleigh peak is associated with the nonpropagating nature of the entropy fluctuation, whereas two shifted Brillouin peaks are associated with adiabatic pressure fluctuations, which propagate as sound waves. Hence, the position of Brillouin peaks is given by the dispersion relation of sound waves. The peak shapes are Lorentzian, and these are broadened due to different dissipative processes, which damp out the fluctuations.

The expressions of the full width at half-maximum (FWHM) for Rayleigh and Brillouin peaks are given by, respectively,

$$W_R = 2 \frac{\Gamma_\chi k}{c_{s0}}, \text{ and } W_B = 2 \frac{\Gamma_\parallel k}{c_{s0}}. \quad (30)$$

The corresponding peak heights are

$$H_R = \frac{4}{W_R} \left(1 - \frac{Q}{\gamma_0}\right), \text{ and } H_B = \frac{2}{W_B} \frac{Q}{\gamma_0}. \quad (31)$$

The total integrated intensity of the Rayleigh peak and each of the two Brillouin peaks are

$$I_R = \left[\frac{\gamma_0 - 1}{\gamma_0} \frac{c_{s0}^2}{c_{\text{eff}}^2} \right] S_{nn}(k) = \left[1 - \frac{Q}{\gamma_0} \right] S_{nn}(k), \quad (32a)$$

$$I_B = \frac{Q}{2\gamma_0} S_{nn}(k). \quad (32b)$$

Thus, $I_R + 2I_B = S_{nn}(k)$, which is a particular case of the sum rule (17). The ratio of the intensity of the central Rayleigh peak to that of the two shifted Brillouin peaks is given by

$$\frac{I_R}{2I_B} = \left(\frac{\gamma_0}{Q} - 1 \right) = (\gamma'_0 - 1). \quad (33)$$

This is known as the Landau-Placzek ratio.

In comparison with the classical hydrodynamic case, the Bohm contribution brings a number of similarities and differences. While the frequency position of the central Rayleigh peak remains unchanged, the frequency positions of the Brillouin peaks are shifted to $\omega = kc_{\text{eff}} \gtrsim kc_{s0}$. Such modified waves are physically similar to sound waves, except for the effective equilibrium pressure being increased by additional quantum pressure arising from the nonlocal Bohm contribution. Most significantly, there are two important modifications: (i) the quantum effects enhance the effective thermal diffusivity by a factor of Q , i.e., $\chi'_0 = Q\chi_0$, and (ii) it reduces the adiabatic index by the same factor of Q , i.e., $\gamma'_0 = \gamma_0/Q$.

For the Rayleigh peak, thermal diffusivity alone determines the width via Γ_χ . With increasing quantum effects, the FWHM of the Rayleigh peak increases due to the enhancement of the effective thermal diffusivity. The height of the Rayleigh peak decreases with increasing quantum effects

because of the combined contributions of the enhanced thermal diffusivity and a reduction in the adiabatic index as per Eq. (31). On the other hand, the width of the Brillouin peak depends on both viscosity and thermal diffusivity via Γ_\parallel , which decreases with increasing quantum effects. It further enhances the height of the Brillouin peak following Eq. (31). These claims are illustrated in Fig. 1.

V. OBLIQUE FLUCTUATIONS

Next, we focus on oblique fluctuations, where the wave vector makes an arbitrary angle, θ , with the magnetic field. The objective is to carry out an analytical calculation for the DSF using the quantum MHD formalism. Through this approach, we aim to gain a comprehensive understanding of the scattering spectrum, considering various combinations of oblique scattering angles, magnetic field strengths, and quantum effects. We then discuss how these factors, along with thermodynamic and transport coefficients, collectively influence the positions and shapes (height and width) of different peaks in the scattering spectra.

The positions of various peaks can be obtained from the roots of $D(k, s)$. By neglecting all the diffusive effects, we find

$$D(k, s) \approx s[s^4 + (k^2 c_{\text{eff}}^2 + k^2 v_A^2) s^2 + k^4 v_A^2 c_{\text{eff}}^2 \cos^2 \theta]. \quad (34)$$

The five roots are then

$$s_* = 0, \quad \pm ikc_F, \quad \pm ikc_S, \quad (35)$$

with associated peak frequencies

$$\omega^2 = 0, \quad k^2 c_F^2, \quad k^2 c_S^2, \quad (36)$$

where

$$c_F = \left[\frac{1}{2} \left\{ (c_{\text{eff}}^2 + v_A^2) + \sqrt{(c_{\text{eff}}^2 + v_A^2)^2 - 4c_{\text{eff}}^2 v_A^2 \cos^2 \theta} \right\} \right]^{1/2}, \quad (37a)$$

$$c_S = \left[\frac{1}{2} \left\{ (c_{\text{eff}}^2 + v_A^2) - \sqrt{(c_{\text{eff}}^2 + v_A^2)^2 - 4c_{\text{eff}}^2 v_A^2 \cos^2 \theta} \right\} \right]^{1/2}. \quad (37b)$$

Using the same approach as for parallel fluctuations, an analytical form of the DSF can be derived using Eq. (16):

$$\begin{aligned} \frac{2\pi S_{nn}(k, \omega)}{S_{nn}(k)} \approx & \left(1 - \frac{Q}{\gamma_0}\right) \left[\frac{2\Gamma_\chi k^2}{\omega^2 + (\Gamma_\chi k^2)^2} \right] + \frac{Q}{\gamma_0} \left[\left(\frac{c_F^2 - v_A^2}{2c_F^2 - v_A^2 - c_{\text{eff}}^2} \right) \left\{ \frac{\Gamma_F k^2}{(\Gamma_F k^2)^2 + (\omega + c_F k)^2} \right. \right. \\ & \left. \left. + \frac{\Gamma_F k^2}{(\Gamma_F k^2)^2 + (\omega - c_F k)^2} \right\} + \left(\frac{c_S^2 - v_A^2}{2c_S^2 - v_A^2 - c_{\text{eff}}^2} \right) \left\{ \frac{\Gamma_S k^2}{(\Gamma_S k^2)^2 + (\omega + c_S k)^2} + \frac{\Gamma_S k^2}{(\Gamma_S k^2)^2 + (\omega - c_S k)^2} \right\} \right], \quad (38) \end{aligned}$$

where

$$\Gamma_F = \frac{1}{2} \left[\left(\frac{c_F^2 - v_A^2}{2c_F^2 - v_A^2 - c_{\text{eff}}^2} \right) (\gamma_0 - Q) \chi_0 + \left(\frac{c_F^2 - c_{\text{eff}}^2}{2c_F^2 - v_A^2 - c_{\text{eff}}^2} \right) \eta_0 + \nu_{s0} + \frac{c_F^2}{c_{\text{eff}}^2} \left(\frac{c_F^2 - v_A^2}{2c_F^2 - v_A^2 - c_{\text{eff}}^2} \right) \nu_{c0} \right], \quad (39a)$$

$$\Gamma_S = \frac{1}{2} \left[\left(\frac{c_S^2 - v_A^2}{2c_S^2 - v_A^2 - c_{\text{eff}}^2} \right) (\gamma_0 - Q) \chi_0 + \left(\frac{c_S^2 - c_{\text{eff}}^2}{2c_S^2 - v_A^2 - c_{\text{eff}}^2} \right) \eta_0 + \nu_{s0} + \frac{c_S^2}{c_{\text{eff}}^2} \left(\frac{c_S^2 - v_A^2}{2c_S^2 - v_A^2 - c_{\text{eff}}^2} \right) \nu_{c0} \right]. \quad (39b)$$

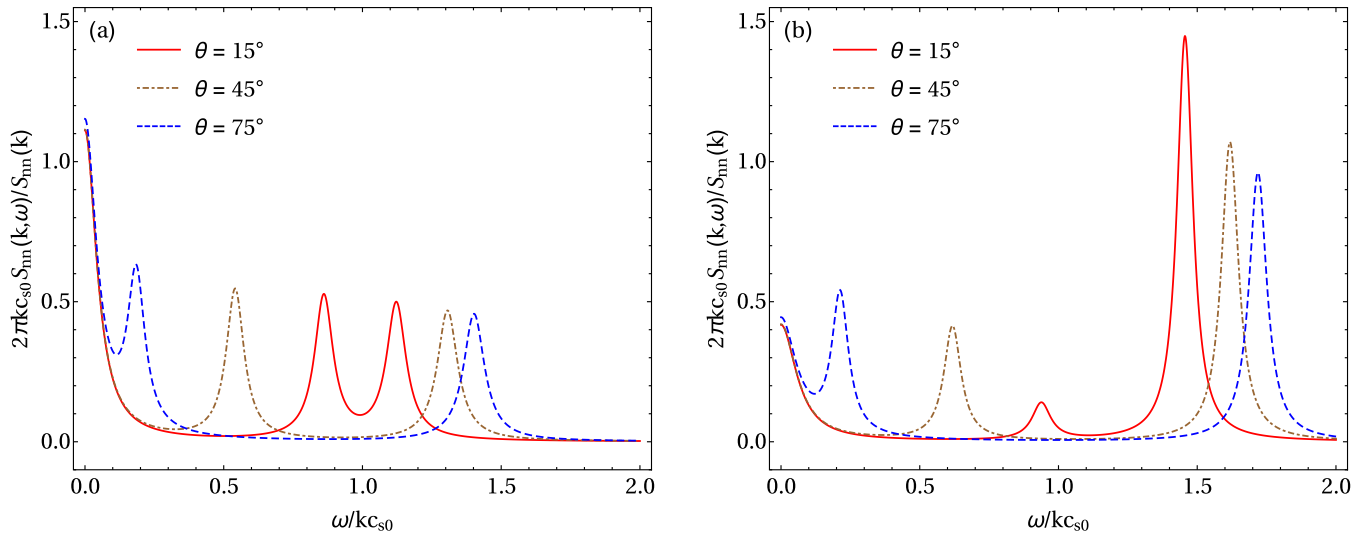


FIG. 2. The dynamic structure factor in magnetized, high density plasma at different oblique scattering angles. The plotted dynamic structure factors are calculated in the same way as in Fig. 1(a), with the same dimensionless values for the dissipative terms. The other parameters are: (a) $c_Q/c_{s0} = 0$, and $v_A/c_{s0} = 1$, and (b) $c_Q/c_{s0} = 1$, and $v_A/c_{s0} = 1$.

For oblique fluctuations, the dynamic structure factor consists of five peaks instead of three. The central Rayleigh peak at $\omega = 0$ remains unchanged, as in the case of pure hydrodynamic or parallel fluctuations. Among the four peaks, there exist a pair of peaks at frequencies $\omega = kc_F \gtrsim kc_{\text{eff}} \gtrsim kc_{s0}$, and a new pair of peaks has emerged at frequencies $\omega = kc_S$. The FWHMs of these different peaks are given by, respectively,

$$W_R = 2 \frac{\Gamma_\chi k}{c_{s0}}, W_F = 2 \frac{\Gamma_F k}{c_{s0}}, \text{ and } W_S = 2 \frac{\Gamma_S k}{c_{s0}}. \quad (40)$$

The width of both pairs of peaks depends on a linear combination of thermal diffusivity, resistivity, and the viscosities via their corresponding Γ 's. The heights of the corresponding peaks are given by

$$H_R = \frac{4}{W_R} \left(1 - \frac{Q}{\gamma_0} \right), \quad (41a)$$

$$H_F = \frac{2}{W_F} \frac{Q}{\gamma_0} \left(\frac{c_F^2 - v_A^2}{2c_F^2 - v_A^2 - c_{\text{eff}}^2} \right), \quad (41b)$$

$$H_S = \frac{2}{W_S} \frac{Q}{\gamma_0} \left(\frac{c_S^2 - v_A^2}{2c_S^2 - v_A^2 - c_{\text{eff}}^2} \right). \quad (41c)$$

Physically, the entropy mode does not contain a magnetic component; thus, the central Rayleigh peak remains unchanged in MHD. The emergence of additional peaks and their characteristics can also be explained physically. Specifically, these peaks correspond to two distinct MHD modes: the fast magnetosonic wave, propagating with a speed c_F , and the slow magnetosonic wave, propagating with a speed c_S . The frequency position of the fast magnetosonic mode is always greater than that for the slow magnetosonic mode. This is because of the effective equilibrium pressure for the fast magnetosonic wave being enhanced by additional magnetic pressure. The amount of enhancement depends on the oblique scattering angle. First, we consider a classical MHD system in which the equilibrium thermal and magnetic energy densities

are comparable; this is equivalent to $v_A = c_{s0}$. In the classical MHD case, the speed associated with the quantum pressure vanishes (i.e., $c_Q = 0$). For quasiperpendicular perturbations (i.e., $\cos \theta \ll 1$), the thermal and magnetic pressure fluctuations are in phase for the fast magnetosonic waves. On the other hand, the slow magnetosonic waves become almost incompressible with thermal and magnetic pressure fluctuations acting out of phase. For the quasiparallel mode (i.e., $\cos \theta \lesssim 1$), the frequencies of the fast and slow magnetosonic modes are of similar orders of magnitude at a given wave number, but the fast mode's frequency is always greater. At positive frequencies, the positions of the fast and slow mode's peak become increasingly separated as θ is increased. These points are illustrated in Fig. 2(a), for a fixed magnetization ($v_A = c_{s0}$) with increasing oblique scattering angles.

In the quantum MHD scenario, we start our analysis by considering the equilibrium quantum speed equating to the equilibrium sound speed, denoted as $c_Q = c_{s0}$. Furthermore, we assume $v_A = c_{s0}$. The resultant DSF is depicted in Fig. 2(b). In comparison to the classical MHD case, due to the introduction of Bohm contributions, the DSF exhibits modified peaks. Quantum effects enhance the effective thermal pressure for both magnetosonic waves. Consequently, the peak positions associated with fast and slow magnetosonic waves shift towards higher frequencies relative to their classical MHD counterparts. Another notable similarity is the increasing separation of peak positions linked to the fast and slow modes as the obliquity angle θ is increased. This behavior primarily stems from the fast mode's peak shifting to a higher frequency and the slow mode's peak shifting to a lower frequency as θ increases, in accordance with Eq. (37). The modification of c_F and c_S with θ directly impacts peak widths through their influence on the corresponding $\Gamma_{F,S}$ [Eq. (39)]. For a given magnetic and quantum pressure, the coefficients associated with various dissipative terms in the expressions for $\Gamma_{F,S}$ change with the opposite sign as the oblique angle changes. Specifically, for the fast mode, the coefficients tied to thermal diffusivity and magnetic diffusivity diminish with

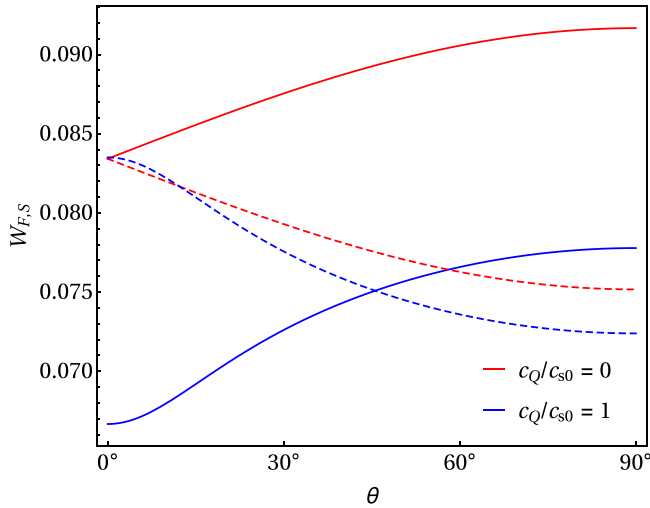


FIG. 3. The FWHM of fast (solid curves) and slow (dashed curves) magnetosonic modes in magnetized, high-density plasma with increasing oblique scattering angles for classical (red curves) and quantum (blue curves) MHD scenarios. We choose $v_A/c_{s0} = 1$. The magnitudes of various dissipative terms are consistent with those in Fig. 1(a).

increasing oblique angle, while the coefficient connected to compressive viscosity increases with rising θ . Consequently, the width of the fast mode peak may either expand or contract, depending on the relative magnitudes of these dissipative terms. For a given set of dissipative terms, the width of the peak linked to the fast mode increases with the oblique angle, as shown in Fig. 3. Conversely, the slow mode experiences a reduction in peak width due to the declining coefficients associated with thermal diffusivity, magnetic diffusivity, and compressive viscosity as θ increases. This is also illustrated in Fig. 3.

In addition to changes in peak width, the peak heights corresponding to the fast and slow modes exhibit diverse

variations as the oblique angle θ changes, while maintaining constant magnetic and quantum pressure conditions, as illustrated in Fig. 2. The peak height is primarily governed by two factors: (i) an inverse relationship with the peak width, and (ii) a dependence on the velocity associated with the corresponding mode, as per Eq. (41). Consequently, as θ increases under fixed magnetic and quantum pressure, the peak height decreases for the fast mode and increases for the slow mode. This behavior remains consistent in both classical [Fig. 2(a)] and quantum [Fig. 2(b)] MHD cases. However, the quantum effects introduce further modifications through the Q factor, which we will discuss in the following paragraph. In Fig. 4, we provide an analysis of the influence of quantum effects on the DSF under the conditions of a constant magnetic pressure and an oblique angle. Figure 4(a) corresponds to the case $v_A/c_{s0} = 1$, and $\theta = 30^\circ$, while Fig. 4(b) is for $v_A/c_{s0} = 0$. The nonmagnetic scenario [Fig. 4(b)] agrees with quantum hydrodynamics [32], with no dependence on the oblique angle θ , thus yielding a DSF identical to that for parallel fluctuations, as illustrated in Fig. 1.

Within the framework of quantum MHD, as depicted in Fig. 4(a), the DSF exhibits five peaks, as previously discussed. The frequency position of the central Rayleigh peak remains unaltered with variations in quantum pressure. Quantum effects, however, enhance the effective thermal pressure for both magnetosonic waves. Consequently, the frequency positions associated with the fast and slow modes shift towards higher frequencies with increasing quantum pressure, as described before. In addition, the Bohm contributions introduce two significant modifications: (i) a reduction of the adiabatic index by a factor of Q , i.e., $\gamma'_0 = \gamma_0/Q$, and (ii) an enhancement of the effective thermal diffusivity by the same factor Q , i.e., $\chi'_0 = Q\chi_0$. Consequently, the product $\gamma_0\chi_0$ remains invariant. This modification is also observed in quantum hydrodynamics (i.e., with no magnetic field present). The increased thermal diffusivity due to quantum effects leads to the broadening of the FWHM of the Rayleigh peak through Γ_χ , resulting in

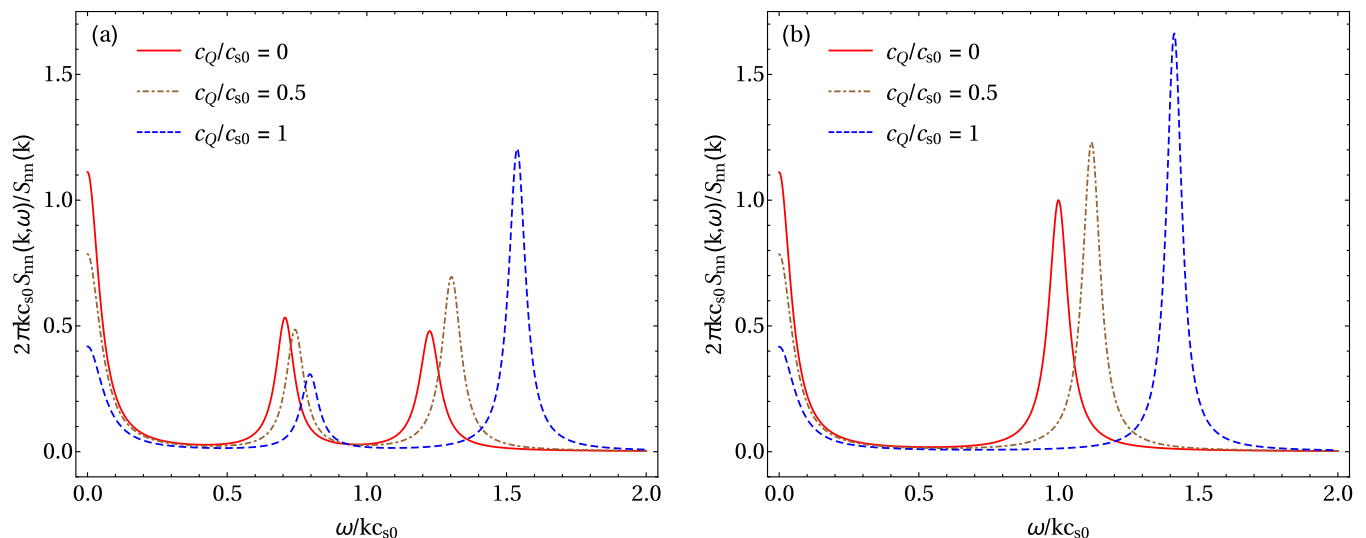


FIG. 4. The dynamic structure factor in magnetized, high-density plasma with increasing quantum effects. The plotted dynamic structure factors are calculated in the same way as in Fig. 1(a), with the same dimensionless values for the dissipative terms. The other parameters are: (a) $v_A/c_{s0} = 1$, and $\theta = 30^\circ$, and (b) $v_A/c_{s0} = 0$, and $\theta \rightarrow$ no role.

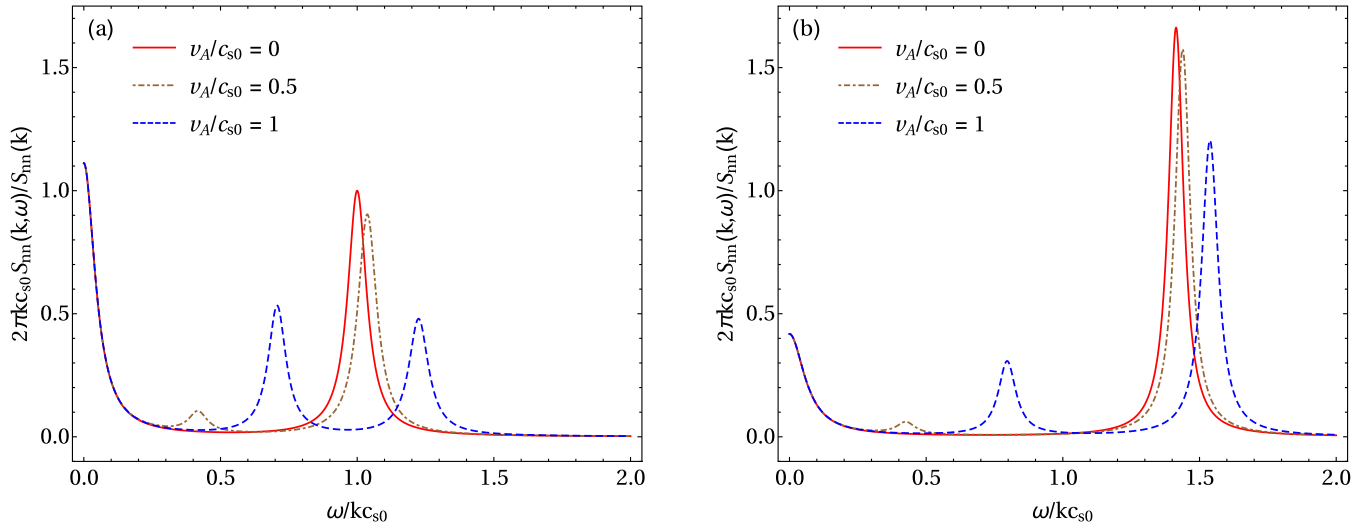


FIG. 5. The dynamic structure factor in magnetized, high-density plasma with increasing magnetization. The plotted dynamic structure factors are calculated in the same way as in Fig. 1(a), with the same dimensionless values for the dissipative terms. The other parameters are: (a) $c_Q/c_{s0} = 0$, and $\theta = 30^\circ$, and (b) $c_Q/c_{s0} = 1$, and $\theta = 30^\circ$.

a reduction in peak height, as explained by Eq. (41a). The width and height of both magnetosonic peaks are determined by a complex interplay of thermal diffusivity, resistivity, and viscosities, following Eqs. (40) and (41), respectively. Similarly, the DSF structures for classical and quantum MHD fluctuations are illustrated in Figs. 5(a) and 5(b), respectively, for a fixed oblique scattering angle ($\theta = 30^\circ$) with increasing magnetization v_A/c_{s0} .

The total integrated intensity of the Rayleigh peak and each of the F- and S-mode peaks are, respectively,

$$I_R = \left[\frac{\gamma_0 - 1}{\gamma_0} \frac{c_{s0}^2}{c_{\text{eff}}^2} \right] S_{nn}(k) = \left[1 - \frac{Q}{\gamma_0} \right] S_{nn}(k), \quad (42a)$$

$$I_F = \frac{1}{2} \left[\frac{Q}{\gamma_0} \left(\frac{c_F^2 - v_A^2}{2c_F^2 - v_A^2 - c_{\text{eff}}^2} \right) \right] S_{nn}(k), \quad (42b)$$

$$I_S = \frac{1}{2} \left[\frac{Q}{\gamma_0} \left(\frac{c_S^2 - v_A^2}{2c_S^2 - v_A^2 - c_{\text{eff}}^2} \right) \right] S_{nn}(k). \quad (42c)$$

Since, $(2c_F^2 - v_A^2 - c_{\text{eff}}^2) = -(2c_S^2 - v_A^2 - c_{\text{eff}}^2) = c_F^2 - c_S^2$, it preserves the sum rule, $I_R + 2I_F + 2I_S = S_{nn}(k)$. The ratio of the intensity of the central Rayleigh peak to that of the four shifted magnetosonic wave peaks is thus given by

$$\frac{I_R}{2I_F + 2I_S} = \left(\frac{\gamma_0}{Q} - 1 \right) = (\gamma'_0 - 1), \quad (43)$$

and it follows the traditional Landau-Placzek ratio. Here, we introduce an additional ratio: the ratio of the intensity of the fast magnetosonic wave peak to that of the slow magnetosonic wave peak,

$$\frac{I_F}{I_S} = \frac{c_F^2 - v_A^2}{v_A^2 - c_S^2} = \frac{c_F^2 - v_A^2}{c_F^2 - c_{\text{eff}}^2}. \quad (44)$$

From an experimental point of view, we note that the F-to-S ratio [Eq. (44)] provides simultaneous sensitivity on both the magnetic field and the effective sound speed, which includes the Bohm contribution, in a magnetized, high-density plasma.

VI. CONCLUSIONS

In this paper, we have derived an analytical expression for the dynamic structure factor in a nonrelativistic, magnetized, high-density quantum plasma. Our approach involves describing collective excitations through the framework of magnetohydrodynamics, in which nonlocal quantum behavior is accounted for through the phenomenological Bohm potential. The inclusion of quantum effects is shown to have noticeable impacts in both hydrodynamics and magnetohydrodynamics conditions. Specifically, the Bohm contributions introduce three significant modifications: (i) an enhancement of the effective thermal pressure, (ii) a reduction of the adiabatic index by a factor of Q , i.e., $\gamma'_0 = \gamma_0/Q$, and (iii) an enhancement of the effective thermal diffusivity by the same factor Q , i.e., $\chi'_0 = Q\chi_0$. It is noteworthy that our analysis leads to the recovery of the same DSF structure as observed in standard classical hydrodynamic fluctuations when $Q = 1$.

In the quantum hydrodynamic case, the DSF is shown to have the same three-peak structure—one central Rayleigh peak and two Brillouin peaks—as in the case of classical hydrodynamic fluctuations, but additional factors related to the quantum Bohm potential are now affecting their position, width, and intensity. The central Rayleigh peak is associated with nonpropagating entropy fluctuations, thus its frequency position remains unchanged. The width of the Rayleigh peak is determined solely by thermal diffusivity through the parameter $\Gamma_\chi = Q\chi_0$, while its height is influenced by both γ'_0 and Γ_χ [Eq. (31)]. For the Brillouin peaks, quantum effects shift the frequency position to a higher frequency due to the enhanced effective thermal pressure from additional quantum pressure. The width of the Brillouin peaks is determined by both thermal diffusivity and viscosity, characterized by the parameter Γ_\parallel [Eq. (27)], while their height is influenced by γ'_0 and Γ_\parallel [Eq. (31)].

In the context of quantum magnetohydrodynamics, the DSF maintains a five-peak structure, featuring a central

TABLE I. Parameters and quantities for plasma diagnostics using the DSF of a magnetized, high-density plasma.

| Parameter/Quantity from DSFs | Description | Plasma Properties |
|--|--|--|
| Peak positions | Associated with two magnetosonic waves | Values for c_F and c_S |
| Landau-Placzek ratio (R_{LP}) | $I_R/(2I_F + 2I_S) = (\gamma'_0 - 1)$ | Adiabatic index (γ'_0) |
| F-to-S ratio (R_{FS}) | $I_F/I_S = (c_F^2 - v_A^2)/(v_A^2 - c_S^2)$ | Alfvén speed (v_A), and hence, magnetic field strength |
| Identity I [obtained from Eq. (37)] | $c_F^2 + c_S^2 = v_A^2 + c_{\text{eff}}^2$ | Speed associated with the effective thermal pressure (c_{eff}) |
| Identity II [obtained from Eq. (37)] | $c_F^2 c_S^2 = v_A^2 c_{\text{eff}}^2 \cos^2 \theta$ | Oblique angle (θ) |
| Width of the central Rayleigh peak via Γ_χ | $\Gamma_\chi = \chi'_0$ | Thermal diffusivity (χ'_0) |
| Width of the fast and slow mode peaks via $\Gamma_{F,S}$ | Expressions given in Eqs. (39a) and (39b) | Correlations ^a between resistivity (η_0) and viscosities (ν_{s0} and ν_{c0}) |

^aNote: It is important to note that the three unknown transport coefficients—resistivity, bulk viscosity and shear viscosity—cannot be simultaneously determined from two known equations [Eqs. (39a) and (39b)], unless one of these coefficients is known to be small.

Rayleigh peak and two pairs of peaks associated with fast and slow magnetosonic waves, as seen in classical magnetohydrodynamic fluctuations [20]. However, the quantum Bohm potential introduces significant alterations, impacting their characteristics, including position, width, and intensity. In MHD, the structure of the DSF is contingent on the angle of fluctuations relative to the prevailing magnetic field within the medium. For fluctuations parallel to the magnetic field, the DSF retains its hydrodynamic nature, as expected. However, oblique fluctuations introduce an extra pair of peaks, associated with magnetic field fluctuations coupled with density fluctuations. Notably, both magnetosonic waves possess significant magnetic and thermal components. The enhancement of effective thermal pressure due to the quantum Bohm potential leads to a shift in the frequency positions of both pairs of peaks towards higher frequencies. Concurrently, resistive, viscous, and conductive dissipative processes dampen fast and slow magnetosonic waves. These damping factors determine the peak width through the respective parameter $\Gamma_{F,S}$, the general expression for which is provided in Eq. (39). The height of these peaks is contingent upon their width (inversely proportional), the modified adiabatic index shaped by quantum effects, and the relative propagation speeds of various waves, following Eq. (41). Finally, the central Rayleigh peak, representing the zero-frequency, nonpropagating entropy mode and devoid of any magnetic component, remains unaltered in MHD.

From an experimental perspective, the presence of multiple peaks in the DSF offers a unique opportunity for the simultaneous measurement of various plasma properties, as well as transport and thermodynamic coefficients in magnetized laboratory plasmas. An important parameter connecting theoretical predictions and experimental observations is the Landau-Placzek ratio, denoted as $R_{LP} = I_R/2I_B = (\gamma_0 - 1)$. This ratio was originally derived from a Rayleigh-Brillouin triplet and provides a direct means to determine the specific heat ratio of diverse liquids and gases through experiments [25–28]. In the context of quantum hydrodynamics, we have found that this ratio modifies to $R_{LP} = I_R/2I_B = (\gamma'_0 - 1)$. For DSFs featuring a five-peak structure, as observed in magnetohydrodynamics, the equivalent form of the Landau-Placzek ratio becomes $I_R/(2I_F + 2I_S) = (\gamma'_0 - 1)$. Additionally, we

introduce another significant ratio known as the F-to-S ratio, denoted as $I_F/I_S = (c_F^2 - v_A^2)/(v_A^2 - c_S^2)$. A suggested strategy for measuring various plasma properties is outlined sequentially in Table I. Hence, the DSF can serve as a robust diagnostic tool for plasma properties that are otherwise very challenging to measure.

ACKNOWLEDGMENTS

The work of G.G. was partially supported by the Science and Technology Facilities Council (STFC) Grant No. ST/W000903/1. T.M. acknowledges support of the Department of Atomic Energy, Government of India, under Project No. RTI4001.

APPENDIX A: QUANTUM POTENTIAL

Here, we follow the original derivation provided by Bohm for a single particle using the representation of the wave function $\psi(\mathbf{x}, t)$ in terms of amplitude $R(\mathbf{x}, t)$ and phase $\phi(\mathbf{x}, t)$, we write [21,22]

$$\psi(\mathbf{x}, t) = R(\mathbf{x}, t)e^{i\phi(\mathbf{x}, t)/\hbar}. \quad (\text{A1})$$

Both $R(\mathbf{x}, t)$ and $\phi(\mathbf{x}, t)$ are real-valued functions of the position vector \mathbf{x} and time t . Employing this ansatz for ψ , the real and imaginary parts of the Schrödinger equation become

$$\frac{\partial \phi}{\partial t} + V_{\text{ext}} + V_Q + \frac{(\nabla \phi)^2}{2m} = 0, \quad (\text{A2a})$$

$$\frac{\partial R^2}{\partial t} + \nabla \cdot \left(R^2 \frac{\nabla \phi}{m} \right) = 0, \quad (\text{A2b})$$

where V_{ext} is the external potential, and

$$V_Q = -\frac{\hbar^2}{2m} \frac{\nabla^2 R}{R}. \quad (\text{A3})$$

Up to this point, Bohm's formalism is exactly equivalent to Schrödinger's description. In correspondence to the classical system, we can treat $R^2 = \rho$ as representing the density of a set of classical systems in configuration space, and $\mathbf{u} = \nabla \phi/m$ as representing the kinetic velocity associated with the wave function ψ . Equation (A2b) thus describes the continuity

equation, while Eq. (A2a) takes the form of a Hamilton-Jacobi equation, with the additional quantum potential given by Eq. (A3). In the classical limit ($\hbar \rightarrow 0$), this additional quantum potential automatically vanishes.

APPENDIX B: THERMODYNAMIC IDENTITIES

In this Appendix, we derive the temperature evolution equation [Eq. (3)] from the internal energy equation [Eq. (1d)]. Here, we also derive Eq. (4) for pressure in terms of state variables density and temperature. Using the first law of thermodynamics and the continuity equation [Eq. (1a)], we write down the internal energy per unit mass as

$$\frac{d\epsilon}{dt} = T \frac{dS}{dt} + \frac{p}{\rho^2} \frac{d\rho}{dt} = T \frac{dS}{dt} - \frac{p}{\rho} \nabla \cdot \mathbf{u}, \quad (\text{B1})$$

where S represents the specific entropy. Substituting Eq. (B1) into Eq. (1d), we obtain a conservation law for specific entropy, as given by

$$\rho T \frac{dS}{dt} = -\mathbf{\Pi} : \nabla \mathbf{u} + \eta \frac{|\nabla \times \mathbf{B}|^2}{\mu_0} - \nabla \cdot \mathbf{q} + \Phi_{\text{Bohm}} \cdot \mathbf{u}. \quad (\text{B2})$$

Assuming that the specific entropy $S = S(\rho, T)$, the total differential is given by

$$dS = \left(\frac{\partial S}{\partial \rho} \right)_T d\rho + \left(\frac{\partial S}{\partial T} \right)_\rho dT. \quad (\text{B3})$$

Applying Maxwell's identities and the first law of thermodynamics, we determine

$$\left(\frac{\partial S}{\partial \rho} \right)_T = -\frac{1}{\rho^2} \left(\frac{\partial p}{\partial T} \right)_\rho = \frac{C_V - C_P}{\alpha_T \rho T}, \quad \left(\frac{\partial S}{\partial T} \right)_\rho = \frac{C_V}{T}, \quad (\text{B4})$$

where C_V is the heat capacity at constant volume, C_P is the heat capacity at constant pressure, and $\alpha_T \equiv -\rho^{-1}(\partial \rho / \partial T)_p$ is the coefficient of thermal expansion. We obtain

$$dS = \frac{C_V}{T} \left(dT - \frac{\gamma - 1}{\alpha_T \rho} d\rho \right), \quad (\text{B5})$$

where we have used $\gamma = C_P/C_V$. Using the continuity equation [Eq. (1a)], we can finally write

$$\frac{dS}{dt} = \frac{C_V}{T} \left(\frac{dT}{dt} - \frac{\gamma - 1}{\alpha_T \rho} \frac{d\rho}{dt} \right) = \frac{C_V}{T} \left(\frac{dT}{dt} + \frac{\gamma - 1}{\alpha_T} \nabla \cdot \mathbf{u} \right). \quad (\text{B6})$$

Substituting Eq. (B6) into Eq. (B2) yields the desired temperature evolution equation [Eq. (3)].

Similarly, for the pressure $p = p(\rho, T)$, we determine the total differential

$$dp = \left(\frac{\partial p}{\partial \rho} \right)_T d\rho + \left(\frac{\partial p}{\partial T} \right)_\rho dT. \quad (\text{B7})$$

Using reciprocity and Maxwell's identities, we obtain

$$\begin{aligned} \left(\frac{\partial p}{\partial \rho} \right)_T &= \frac{C_V}{C_P} \left(\frac{\partial p}{\partial \rho} \right)_S = \frac{c_s^2}{\gamma}, \\ \left(\frac{\partial p}{\partial T} \right)_\rho &= - \left(\frac{\partial p}{\partial \rho} \right)_T \left(\frac{\partial \rho}{\partial T} \right)_p = \frac{c_s^2}{\gamma} \rho \alpha_T, \end{aligned} \quad (\text{B8})$$

where $c_s^2 \equiv (\partial p / \partial \rho)_S$ represents the adiabatic sound speed. These expressions lead to the final expression

$$dp = \frac{c_s^2}{\gamma} (d\rho + \rho \alpha_T dT), \quad (\text{B9})$$

from which Eq. (4) follows trivially.

-
- [1] S. Ichimaru, Strongly coupled plasmas: high-density classical plasmas and degenerate electron liquids, *Rev. Mod. Phys.* **54**, 1017 (1982).
- [2] P. K. Shukla and B. Eliasson, Colloquium: Nonlinear collective interactions in quantum plasmas with degenerate electron fluids, *Rev. Mod. Phys.* **83**, 885 (2011).
- [3] J. Daligault and S. Gupta, Electron-ion scattering in dense multi-component plasmas: Application to the outer crust of an accreting neutron star, *Astrophys. J.* **703**, 994 (2009).
- [4] A. K. Harding and D. Lai, Physics of strongly magnetized neutron stars, *Rep. Prog. Phys.* **69**, 2631 (2006).
- [5] T. Mondal, The life cycle of magnetars: A novel approach to estimate their ages, *Astrophys. J. Lett.* **913**, L12 (2021).
- [6] T. Guillot, Interior of Giant Planets Inside and Outside the Solar System, *Science* **286**, 72 (1999).
- [7] R. F. Smith *et al.*, Equation of state of iron under core conditions of large rocky exoplanets, *Nature Astron.* **2**, 452 (2018).
- [8] L. Bildsten and D. M. Hall, Gravitational settling of ^{22}Ne in liquid white dwarf interiors, *Astrophys. J. Lett.* **549**, L219 (2001).
- [9] U. Das and B. Mukhopadhyay, New mass limit for white dwarfs: Super-chandrasekhar type Ia supernova as a new standard candle, *Phys. Rev. Lett.* **110**, 071102 (2013).
- [10] A. Becker, W. Lorenzen, J. J. Fortney, N. Nettelmann, M. Schöttler, and R. Redmer, *Ab Initio* Equations of State for Hydrogen (H-REOS.3) and Helium (He-REOS.3) and their Implications for the Interior of Brown Dwarfs, *Astrophys. J. Suppl. Ser.* **215**, 21 (2014).
- [11] J. D. Lindl, P. Amendt, R. L. Berger, S. G. Glendinning, S. H. Glenzer, S. W. Haan, R. L. Kauffman, O. L. Landen, and L. J. Suter, The physics basis for ignition using indirect-drive targets on the National Ignition Facility, *Phys. Plasmas* **11**, 339 (2004).
- [12] J. A. Gaffney *et al.*, A Review of Equation-of-State Models for Inertial Confinement Fusion Materials, *High Energy Density Phys.* **28**, 7 (2018).
- [13] J. Hansen and I. McDonald, *Theory of Simple Liquids* (Elsevier Academic Press, Amsterdam, 2013).
- [14] S. H. Glenzer and R. Redmer, X-ray Thomson scattering in high energy density plasmas, *Rev. Mod. Phys.* **81**, 1625 (2009).
- [15] J. P. Mithen, J. Daligault, and G. Gregori, Extent of validity of the hydrodynamic description of ions in dense plasmas, *Phys. Rev. E* **83**, 015401(R) (2011).
- [16] J. P. Mithen, J. Daligault, B. J. B. Crowley, and G. Gregori, Density fluctuations in the Yukawa one-component plasma: An

- accurate model for the dynamical structure factor, *Phys. Rev. E* **84**, 046401 (2011).
- [17] E. E. Salpeter, Plasma density fluctuations in a magnetic field, *Phys. Rev.* **122**, 1663 (1961).
- [18] J. Sheffield, D. Froula, S. Glenzer, and N. Luhmann, *Plasma Scattering of Electromagnetic Radiation: Theory and Measurement Techniques* (Elsevier Science, Amsterdam, 2010).
- [19] H. Herold, Compton and Thomson scattering in strong magnetic fields, *Phys. Rev. D* **19**, 2868 (1979).
- [20] A. F. A. Bott and G. Gregori, Thomson scattering cross section in a magnetized, high-density plasma, *Phys. Rev. E* **99**, 063204 (2019).
- [21] D. Bohm, A suggested interpretation of the quantum theory in terms of “Hidden” variables. I, *Phys. Rev.* **85**, 166 (1952).
- [22] F. Haas, *Quantum Plasmas: An Hydrodynamic Approach*, Springer Series on Atomic, Optical, and Plasma Physics, Vol. 65 (Springer, New York, 2011).
- [23] B. Larder, D. O. Gericke, S. Richardson, P. Mabey, T. G. White, and G. Gregori, Fast nonadiabatic dynamics of many-body quantum systems, *Sci. Adv.* **5**, eaaw1634 (2019).
- [24] M. Bonitz, Z. A. Moldabekov, and T. S. Ramazanov, Quantum hydrodynamics for plasmas—Quo vadis? *Phys. Plasmas* **26**, 090601 (2019).
- [25] H. Z. Cummins and R. W. Gammon, Rayleigh and Brillouin scattering in liquids: The Landau—Placzek ratio, *J. Chem. Phys.* **44**, 2785 (1966).
- [26] C. L. O’Connor and J. P. Schlupf, Brillouin scattering in water: The Landau-Placzek ratio, *J. Chem. Phys.* **47**, 31 (1967).
- [27] V. A. Popova and N. V. Surovtsev, Temperature dependence of the Landau-Placzek ratio in glass forming liquids, *J. Chem. Phys.* **135**, 134510 (2011).
- [28] V. A. Zykova, Y. A. Karpegina, V. K. Malinovsky, and N. V. Surovtsev, Temperature dependence of the Landau-Placzek ratio in liquid water, *Phys. Rev. E* **96**, 042608 (2017).
- [29] F. Haas, A magnetohydrodynamic model for quantum plasmas, *Phys. Plasmas* **12**, 062117 (2005).
- [30] S. Chapman and T. G. Cowling, *The Mathematical Theory of Non-Uniform Gases* (Cambridge University Press, Cambridge, 1970).
- [31] J. E. Cross, B. Reville, and G. Gregori, Scaling of magneto-quantum-radiative hydrodynamic equations: From laser-produced plasmas to astrophysics, *Astrophys. J.* **795**, 59 (2014).
- [32] R. Schmidt, B. J. B. Crowley, J. Mithen, and G. Gregori, Quantum hydrodynamics of strongly coupled electron fluids, *Phys. Rev. E* **85**, 046408 (2012).